Prediction of Bilinear Stress-Strain Curve of Thin Hard Coating by Nanoindentation Test and Finite Element Method

T. S. Yang, Y. Y. Chang, and S. Y. Chang

Abstract—**This study applies the finite element method (FEM) in conjunction with an nanoindentation test to predict bilinear stress-strain curve of thin hard coatings. To verify the prediction of FEM simulation for loading and unloading process, the experimental data are compared with the results of current simulation. Loading curve is investigated for different material parameters, such as elastic modulus *E*, yield stress Y_0 and tangent modulus *ET* of nanoindentation process, by finite element analysis. The effects of material properties of thin film on the stress distribution for loading and unloading in the nanoindentation are also investigated. Finally, the bilinear stress-strain curve of thin hard coatings is directly extracted by comparing of loading curves between FEM simulation results and nanoindentation test results.**

Index Terms—**Finite element method, nanoindentation test, bilinear stress-strain curve**

I. Introduction

Finite element method (FEM) has been widely used for numerical simulation of indentation tests on bulk and film material in order to analyze its deformation response and investigate the influence of indenter geometry, friction and material elastic and plastic properties. The Brinell test [1], in a form of indentation test, expands the loading type to nano ranges depending on the materials and applications. Pelletier et. al [2] have investigated the influence of material bilinear elastic-plastic behaviour model for numerical simulation of nanoindentation testing of various bulk metals. The indenter and the specimen were treated as a revolution body in order to have three-dimensional situation. The numerical simulation results of loads verse displacement compare reasonable well to experimental results of nanoindentation tests of pure metals as Fe, Ni, Ti and Cu. Pelletier [3] used a comprehensive parametric study of 48 cases was conducted. They defined two dimensionless equations which link the parameters extracted from the experimental load–displacement curve with material parameters, such as Young's modulus, yield stress and tangent modulus. The

load–displacement curves simulated by FEM and then experimental curves obtained by nanoindentation testing using a Berkovich tip. Bhattacharya and Nix et. al. [4] used the finite element (FE) method to simulate and solve for an indentation problem with an axisymmetric cone. The results compared well with experimental data. They presented an elasto-plastic analysis of axisymmetric conical indentation, and showed that the shape of the plastic zone strongly depends on the indenter angle, Young's modulus of the material, and yield stress. Khan et al. [5] used nanoindentation test and finite element analysis to extract yield stress and strain hardening exponent for an Al-clad system. Through nanoindentation properties including maximum load of indentation, contact depth, area of contact and pile-up obtained from the forward and reverse analyses showed excellent agreement with the experimental results. Adam and Swain [6] investigated the changes in friction coefficient at the interface between indenter and bone strongly affects predicted pile-up in nanoindentation simulations of bone.

This study applies the finite element method (FEM) in conjunction with a nanoindentation test to predict bilinear stress-strain curve of film metal during the nanoindentation process. To verify the prediction of FEM simulation for loading and unloading process, the experimental data are compared with the results of current simulation. Loading-unloading curve is investigated for different material parameters, such as elastic modulus *E*, yield stress Y_0 and tangent modulus *ET* of nanoindentation process, by finite element analysis. The effects of material properties of thin film on the stress distribution for loading and unloading in the nanoindentation are also investigated. Finally, the bilinear stress-strain behavior of a local region of a material is directly extracted by the comparison of loading curves between the FEM simulation and a nanoindentation test.

II. Finite Element Indentation Simulations

A. Basic theory of DEFROM

This study applies commercial finite element code DEFORM-2D [7] to simulate the elasto-plastic deformation behavior during the indentation process. The basic equations of the finite element analysis are as follows:

$$\pi = \int_v \overline{\sigma}\, \dot{\overline{\varepsilon}}\, dv \; - \; \int_s F_i u_i\, ds \tag{1}$$

where is the effective stress, is the effective strain-rate,

S. Y. Chang is with the National Formosa University, Yunlin, 63201 Taiwan, (corresponding author to provide phone: +886-5-631-5323; fax:+886-5-631-5310; e-mail: kim1025.tw@yahoo.com.tw).
T. S. Yang is with the National Formosa University, Yunlin, 63201 Taiwan, (e-mail: tsyang@nfu.edu.tw).
Y. Y. Chang is with the National Formosa University, Yunlin, 63201 Taiwan, (e-mail: yinyu@nfu.edu.tw).

Fi represents the surface tractions and, ui is the velocity components. The variational form for finite-element discretization is given by:

$$\delta\pi = \int_v \overline{\sigma}\,\delta\,\dot{\overline{\varepsilon}}\,dv + k\int_v \dot{\varepsilon}_v \delta\,\dot{\varepsilon}_v\,dv - \int_s F_i \delta u_i ds = 0 \qquad (2)$$

where $\dot{\varepsilon}_v = \dot{\varepsilon}_{ii}$ is the volumetric strain rate, π is functional of the total energy and work, and k, a penalty constant, is a very large positive constant. $\delta\dot{\overline{\varepsilon}}$ and $\delta\dot{\varepsilon}_v$ are the variations in effective strain rate and volumetric strain rate. The Newton-Raphson iteration method is applied to obtain the solution of the equations. The convergence criteria for the iteration are the velocity error norm $\|\Delta v\|/\|v\| \le 0.01$ and the force error norm $\|\Delta F\|/\|F\| \le 0.1$, where $\|v\|$ is defined as $(v^T v)^{1/2}$.

B. Basic theory of nanoindentation test

In the Oliver and Pharr method, the hardness H and the reduced modulus E_r are derived from

$$H = \frac{P_{max}}{A(h_c)} \qquad (3)$$

and

$$S = 2\beta\sqrt{\frac{A}{\pi}}E_\gamma \qquad (4)$$

where P_{max} is the maximum indentation load, A is the projected contact area, S is the unloading stiffness measured at maximum depth of penetration h, β is a constant that depends on the geometry of the indenter, for Berkovich indenter $\beta=1.034$. The reduced modulus is used in the analysis to take into account that elastic deformation occurs in both the indenter and the specimen and it is given by

$$\frac{1}{E_\gamma} = \frac{1-v^2}{E} + \frac{1-v_i^2}{E_i} \qquad (5)$$

where E, E_i and v, v_i are the elastic modulus and Poisson's ratio of the indenter and the specimen material, respectively. For evaluating the elastic modulus E_γ, the unloading stiffness

$$S = \frac{dP}{dh}\bigg|_{P_{max}} \qquad (6)$$

the Berkovich diamond tip was used and be simulated as a perfectly elastic material with elastic modulus of 1140 GPa and Poisson' ratio of 0.07.

C. Finite element indentation models

Figure 1 shows the FE-model of the film-substrate system on the nanoindentation process simulated in DEFORM-2D. An axisymmetric cone with half-included angle of 70.3° in which the conical indenter has the same area function as a Berkovich tip was used. The movement of the indenter is constrained to within the thickness-direction of the film

metal. Nanoindentation is performed under precise and continuous load and depth measurement during the loading and unloading process (Fig. 2(a)). Figure 2(b) presents the stress-strain curve with bilinear constitutive law of a film material where E is the elastic modulus, Y_0 is the yield stress, and ET is the tangent modulus. The analyses assume that the substrate and indenter are elastic-plastic and rigid. Only half of the indenter and bulk material was simulated since both the indenter and material were symmetrical. The nodes along the axis of rotation can move only along the y-axis and all nodes on the bottom of the mesh are fixed. The meshes near the indenter must be sufficiently fine to describe the deformation and stress gradient below the indenter with sufficient accuracy. The analysis assumed a frictionless interface between the indenter and the specimen. The model adopts 4-node tetrahedral elements for the substrate and film materials in two-dimensional simulation. The proper size of the meshes for the FE models is determined through convergence studies. The substrate and film materials are meshed about 973 elements, 1037 nodes and 1000 elements, 1058 nodes, respectively. The indentation process is simulated during both loading and unloading. During the loading process, the load corresponding to the applied depth is calculated by summing the resistant force at the bottom nodes of the specimen, which is equivalent to the indenter force. FE simulation of the unloading process is performed by returning the applied indenter to its original position by controlling the indenter depth. The reaction load versus depth of the indenter is taken as measures representing the material system response.
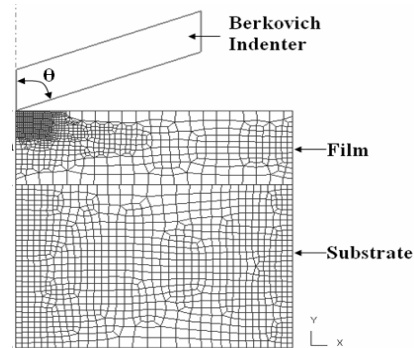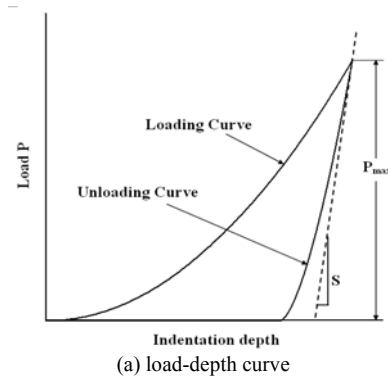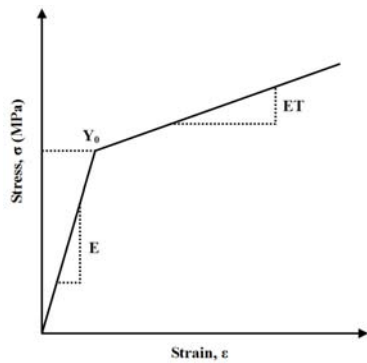

Fig 1 The configuration of indenter, film and substrate during nanoindentation finite element simulation.

(a) load-depth curve

(b) bilinear stress-strain curve

Fig. 2. Schematic of the (a) load-depth curve and (b) bilinear stress-strain curve.

D. Parametric FE indentation simulations

To verify the FEM simulation results obtained by DEFORM-2D software for the load and unload curve of bulk and film metal during the nanoindentation process, experimental data obtained by Pelletier et al. [2] are compared with simulation results obtained by this study. The experimental conditions in Pelletier et al. [2] are adopted as the simulation input parameters. Figure 3 shows the comparison between the current simulation and the results of Pelletier et al. [2] for loading and unloading curves of *Al* metal and material *F2*. The results predicted by present simulation are in good agreement with FE simulation Therefore, the DEFORM-2D can effectively capture the loading and unloading curves in nanoindentation process.
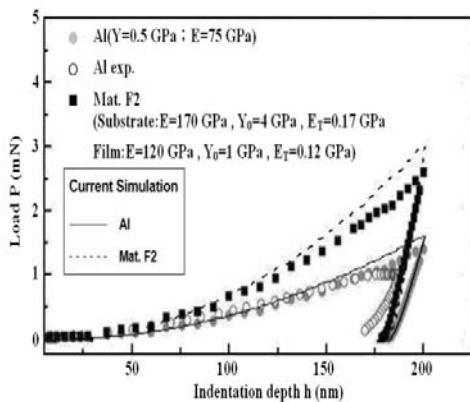

Fig. 3. Comparison between current simulations and experimental results of Pelletier et al. [2]

The effects of material parameters of the films, *i.e.,* elastic modulus E, yield stress Y_0 and tangent modulus ET on the loading curve of film on substrate composites, were measured by performing numerical analyses of each change in these values. The substrate and film material have thicknesses of 2 mm and 900 nm, respectively. Indentation depth is 300 nm. Figure 4 shows the effect of the elastic modulus E of thin hard coating on the loading curve for the nanoindentation process. The figure shows that the maximum load values at the indenter tip increased from 6.46 mN to 8.03 mN when the elastic modulus of thin film was increased from 72 GPa to 700 GPa. The large values of elastic modulus of thin hard coating result in high maximum indentation load values. Figure 5 shows the effect of yield stress Y_0 for the thin hard coating on the loading curve for the nanoindentation

process. The figure shows that the maximum load values at the location of indenter tip increased from 7.41 mN to 9 mN as overall yield stress of thin film increased from 100 MPa to 800 MPa. The large yield stress values for the thin hard coating result in high maximum indentation load values. Figure 6 shows the effect of the tangent modulus ET of thin hard coating on the loading curve for the nanoindentation process. According to the figure, the maximum values of load at the location of indenter tip increased from 4.46 mN to 10.5 mN as the tangent modulus of thin film was increased from 3.6 GPa to 50 GPa, respectively. The large tangent modulus values for the thin hard coating result in high values of maximum indentation load.
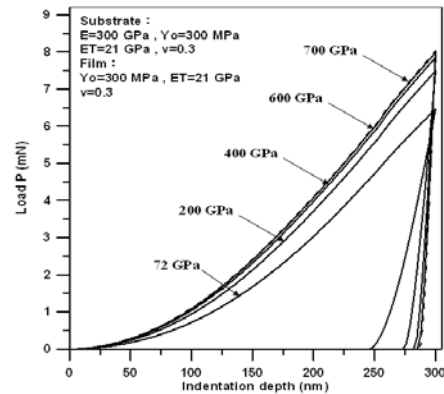

Fig. 4. Effect of Elastic modulus of thin film on the loading curve in the nanoindentation.
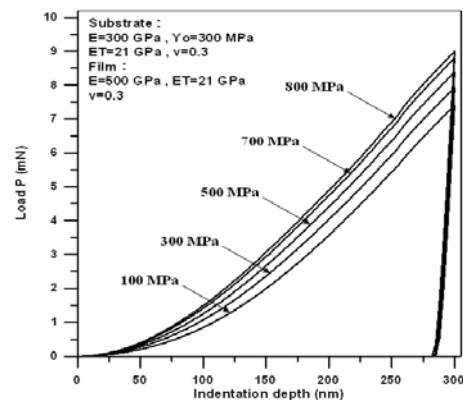

Fig. 5. Effect of Yield stress of thin film on the loading curve in the nanoindentation.
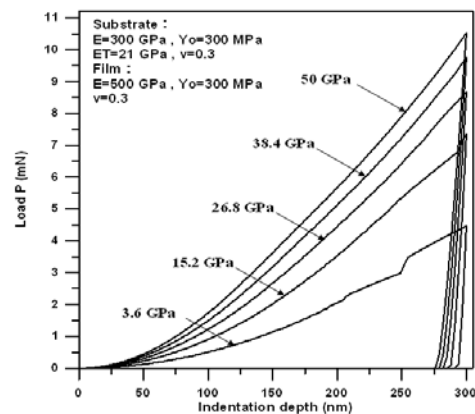

Fig.6. Effect of Tangent modulus of thin film on the loading curve in the nanoindentation.

The effects of material parameters of the films, *i.e.,* elastic modulus E, yield stress Y_0 and tangent modulus ET on the stress distribution of film on substrate composites for loading and unloading, were measured by performing numerical analyses of each change in these values. Figures 7(a), (b) and (c) show the effect of the elastic modulus of film on the effective stress distribution for loading and unloading in nanoindentation under the condition of ET =21 GPa, and Y_0 =300 MPa of film. The material property of substrate is E =300 GPa, ET =21 GPa, and Y_0 =300 MPa. The maximum value of the effective stress is approximately 15.5, 17.5, and 17.5MPa for 72, 400, and 700 GPa elastic modulus in loading process, respectively. The maximum value of the effective stress is approximately 2.09, 2.96, and 3.63MPa for 72, 400, and 700 GPa elastic modulus in unloading process, respectively. The maximum values of the effective stress for different film elastic modulus in loading and unloading are shown in Table 1. Figures 8(a), (b) and (c) show the effect of the yield stress of film on the effective stress distribution for loading and unloading in nanoindentation under the condition of E =500 GPa, and ET =21 GPa of film. The material property of substrate is E =300 GPa, ET =21 GPa, and Y_0 =300 MPa. The maximum value of the effective stress is approximately 17.3, 17.8, and 19.0MPa for 100, 400, and 800 MPa yield stress in loading process, respectively. The maximum value of the effective stress is approximately 2.98, 3.32, and 3.75MPa for 100, 400, and 800 MPa yield stress in unloading process, respectively. The maximum values of the effective stress for different film yield stress in loading and unloading are shown in Table 2. Figures 9(a), (b) and (c) show the effect of the yield stress of film on the effective stress distribution for loading and unloading in nanoindentation under the condition of E =500 GPa, and Y_0 =300 MPa of film. The material property of substrate is E =300 GPa, ET =21 GPa, and Y_0 =300 MPa. The maximum value of the effective stress is approximately 6.68, 19.9, and 28.5 MPa for 3.6, 26.8, and 50 GPa tangent modulus in loading process, respectively. The maximum value of the effective stress is approximately 1.97, 3.4, and 4.78MPa for 3.6, 26.8, and 50 GPa tangent modulus in unloading process, respectively. The maximum values of the effective stress for different film tangent modulus in loading and unloading are shown in Table 3.

(a) stress distribution for loading and unloading (E=72 GPa)

(b) stress distribution for loading and unloading (E=400 GPa)

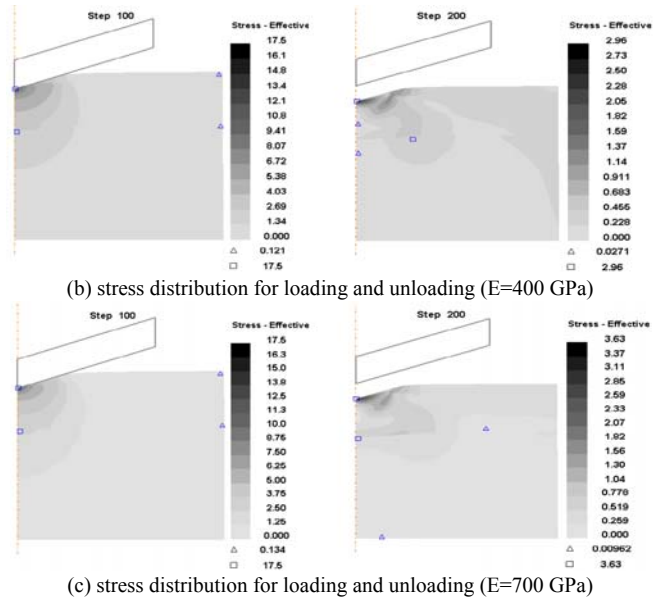(c) stress distribution for loading and unloading (E=700 GPa)

Fig. 7. Effect of Elastic modulus of thin film on the stress distribution for loading and unloading in the nanoindentation.

Table 1. Maximum values of the effective stress for different film elastic modulus.

Substrate	E=300 GPa, E_T=21 GPa, Y_0=300 MPa		
Film	E_T=21 GPa, Y_0=300 MPa		
	E	Max. effective stress (MPa)	
	(GPa)	Loading	Unloading
	72	15.5	2.09
	400	17.5	2.96
	700	17.5	3.63

(a) stress distribution for loading and unloading (Y_0=100 MPa)

(b) stress distribution for loading and unloading (Y_0=400 MPa)

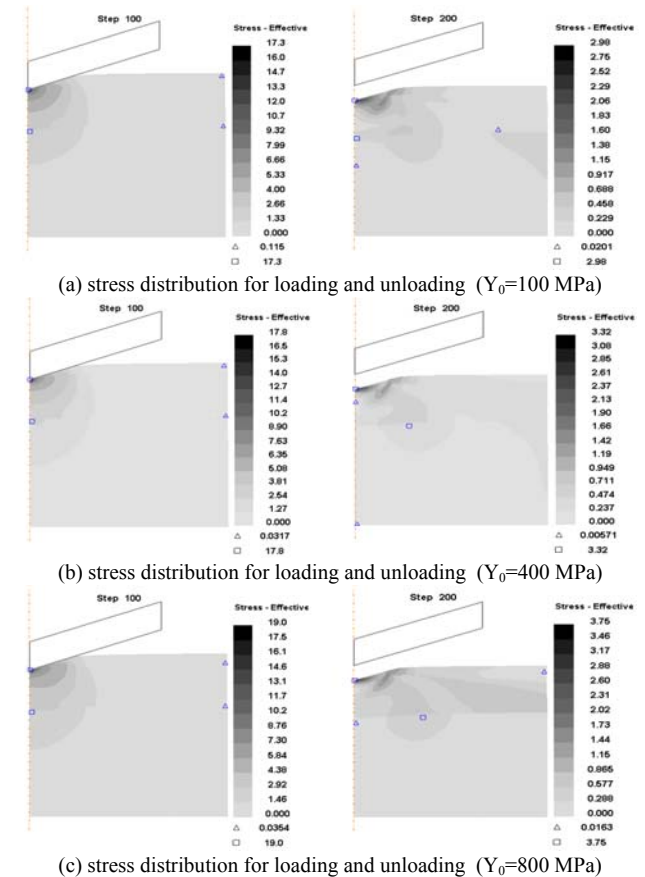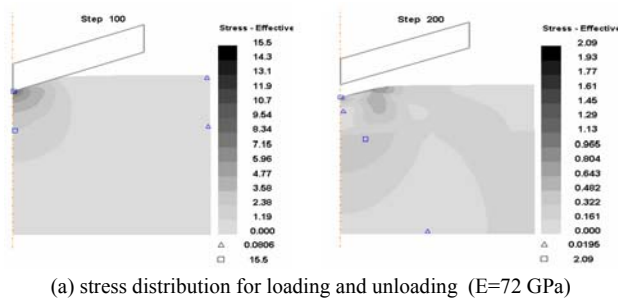(c) stress distribution for loading and unloading (Y_0=800 MPa)

Fig. 8. Effect of Yield stress of thin film on the stress distribution for loading and unloading in the nanoindentation.

Table 2. Maximum values of the effective stress for different film yield stress.

Substrate	E=300 GPa, E_T=21 GPa, Y_0=300 MPa		
Film	E=500 GPa, E_T=21 GPa		
	Y_0	Effective Stress (MPa)	
	(MPa)	Loading	Unloading
	100	17.3	2.98
	400	17.8	3.32
	800	19	3.75

(a) stress distribution for loading and unloading (E_T=3.6 GPa)

(b) stress distribution for loading and unloading (E_T=26.8 GPa)

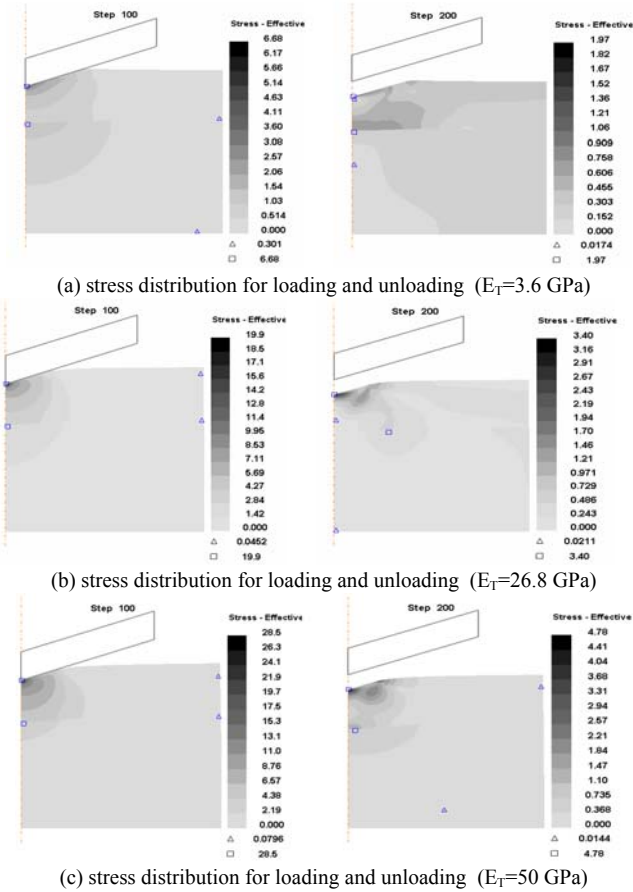(c) stress distribution for loading and unloading (E_T=50 GPa)

Fig. 9. Effect of Tangent modulus of thin film on the stress distribution for loading and unloading in the nanoindentation.

Table 3. Maximum values of the effective stress for different film tangent modulus.

Substrate	E=300 GPa, E_T=21 GPa, Y_0=300 MPa		
Film	E=500 GPa, Y_0=300 MPa		
	E_T	Effective Stress (MPa)	
	(GPa)	Load	Unloading
	3.6	6.68	1.97
	26.8	19.9	3.4
	50	28.5	4.78

III. DETERMINE THE BILINEAR STRESS-STRAIN CURVE FOR THE THIN HARD COATING

A. Flow chart of procedure for constructing bilinear stress-strain curve

Figure 10 shows the flow chart to determine the bilinear stress-strain curve. First, the elastic modulus maximum load

and load-depth curve for the coating are obtained based on the nanoindentation test measurements. By comparing the maximum load of the simulation and experimental results and make them closely, then, each tangent modulus is obtained. Deform-2D was again used to simulate the above parameters to obtain different material properties of the load-depth curve. The simulated load-depth curve was used for comparison with the experimental results. A set of simulation curves and experimental curves that are in good agreement confirms that this set of simulation parameters for the curve accurately corresponds with the material properties of the coating.
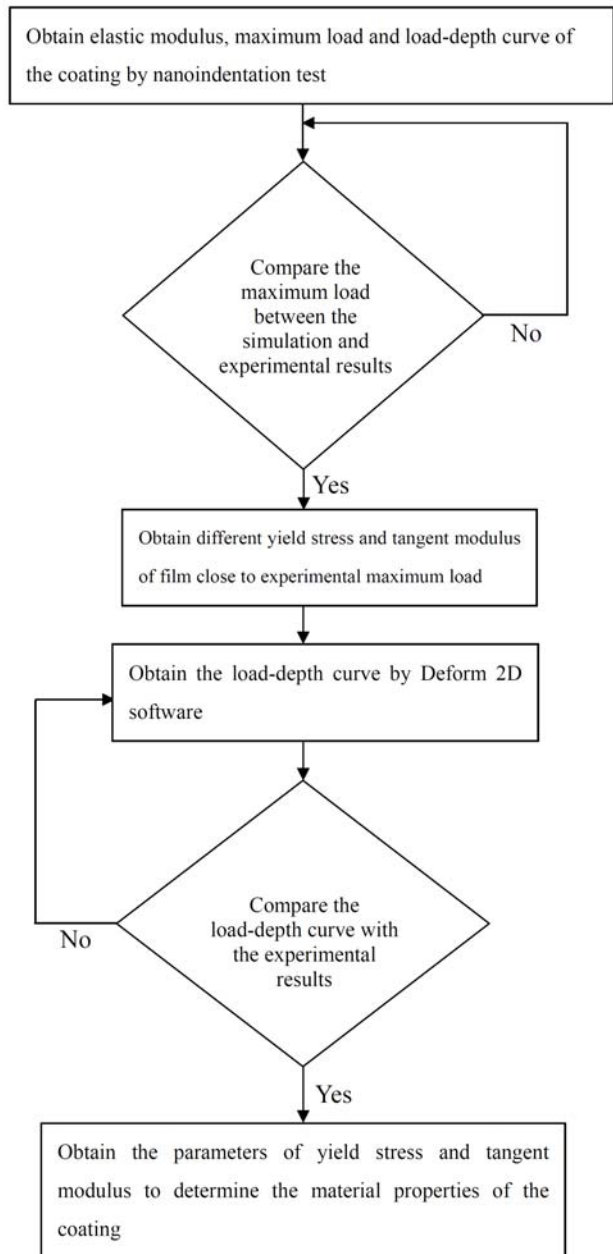

Fig. 10. Flow chart for constructing the bilinear stress-strain curve.

B. Results

Fig. 11 shows the loading and unloading curve for substrate (Si) and film (Cu). The elastic modulus is 133 GPa of substrate and the elastic modulus is 169 GPa of film. The maximum load (3.198 mN) of the Cu film was obtained by nanoindentation test. The first set material properties of film are Y_0 =35 MPa, and ET =4.175 GPa. The secocond set

material properties of film are Y_0 =212 MPa, and ET =1.620 GPa. The third set material properties of film are Y_0 =333 MPa, and ET =0.387 GPa. The simulation of the maximum load close to the experimental resullt (3.198 mN) in each set. But the simulation result of loading curve of third set material properties(Y_0 =333 MPa, and ET =0.387 GPa) close to experimental data. According to the simulation results, the material parameters for the Cu film were elastic modulus about 169 GPa, yield stress about 333 MPa, and tangent modulus about 0.387 GPa. Fig. 12 shows the loading and unloading curve for Mat. F2. The elastic modulus is 170 GPa of substrate and the elastic modulus is 120 GPa of film. The maximum load (2.610 mN) of the Cu film was obtained by nanoindentation test. The first set material properties of film are Y_0 =125 MPa, and ET = 12.044 GPa. The secocond set material properties of film are Y_0 = 469 MPa, and ET =5.120 GPa. The third set material properties of film are Y_0 =701 MPa, and ET =1.412 GPa. The simulation of the maximum load close to the experimental resullt (2.610 mN) in each set. But the simulation result of loading curve of third set material properties(Y_0 =701 MPa, and ET =1.412 GPa) close to experimental data. According to the simulation results, the material parameters for the film were elastic modulus about 120 GPa, yield stress about 701 MPa, and tangent modulus about 1.412 GPa.
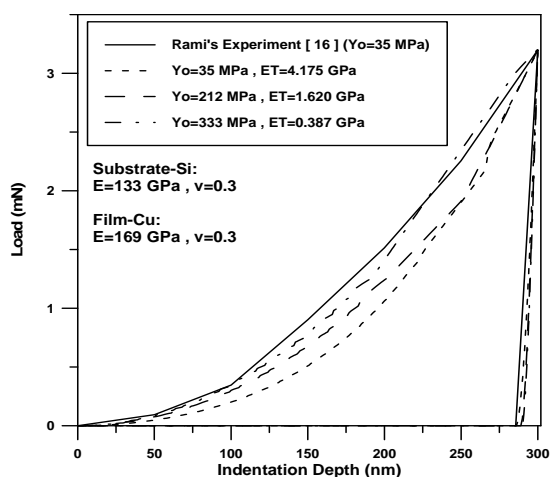

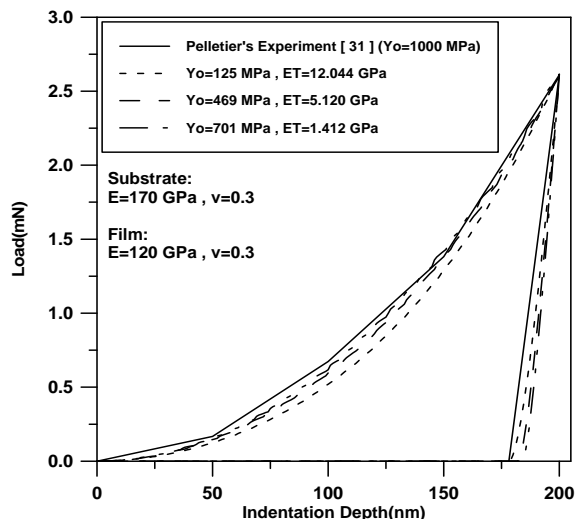Fig. 11. Loading and unloading curve for substrate (Si) and film (Cu).

Fig. 12. Loading and unloading curve for the Mat. F2.

IV. CONCLUSION

Finite element analysis was performed to simulate the effects of material parameters such as elastic modulus, yield stress, and tangent modulus on the maximum nanoindentation load. The larger values of the elastic modulus, yield stress and tangent modulus of coatings had the higher maximum load. The Effect of material properties of thin film on the stress distribution for loading and unloading in the nanoindentation are also investigated. So far, the nanoindentation test can only obtain the elastic modulus and no other mechanical properties. This study provides an approach to measure other mechanical properties of film such as yield stress and tangent modulus. The mechanical properties of the two films (Cu and Mat. F2) are confirmed by comparing the experimental data with the simulation results.

REFERENCES

[1] D. Tabor, Indentation hardness: fifty years on a personal view, Philos. Mag. A, vol. 74, pp. 1207-21, 1996.
[2] H. Pelletier, J. Krier, A. Cornet, P. Mille, Limits of using bilinear stress-strain curve for finite element modeling of nanoindentation response on bulk materials, Thin Solid Films. vol. 379, pp. 147-155, 2000.
[3] H. Pelletier, Predictive model to estimate the stress–strain curves of bulk metals using nanoindentation, Tribology International. vol. 39, pp. 593-606, 2006.
[4] A. K. Bhattacharya, W. D. Nix, Finite element analysis of cone indentation, International Journal of Solids and Structure. vol. 27, pp. 1047-1058, 1991.
[5] M.K. Khan, S.V. Hainsworth, M.E. Fitzpatrick, L. Edwards, A combined experimental and finite element approach for determining mechanical properties of aluminium alloys by nanoindentation, Computational Materials Science. vol. 49, pp. 751-760, 2010.
[6] C.J. Adama, M.V. Swain, The effect of friction on indenter force and pile-up in numerical simulations of bone nanoindentation, Journal of the mechanical behavior of biomedical materials. vol. 4, pp. 1554-1558, 2011.
[7] Anon. *DEFORM-2D Version 9.0 User Manual*, Columbus, Ohio: Scientific Forming Technologies Corporation. 2006.